Cholesteric Monomer and Elastomers Containing Menthyl Groups: Synthesis and Phase Behavior

Jian-She Hu, Dan Li, Qing-Bao Meng, Dan-Shu Yao

Center for Molecular Science and Engineering, College of Science, Northeastern University, Shenyang 110004, People's Republic of China

Received 14 August 2011; accepted 22 December 2011
DOI 10.1002/app.36701
Published online in Wiley Online Library (wileyonlinelibrary.com).

ABSTRACT: The synthesis of a new cholesteric monomer ($\mathbf{M_{LC}}$) containing menthyl groups and a series of cholesteric elastomers ($\mathbf{LCE_1}$–$\mathbf{LCE_4}$) is described. Their chemical structures and purity were characterized by FTIR, ^{1}H-NMR, and elemental analyses. The phase behavior and thermal stability were investigated by differential scanning calorimetry, polarizing optical microscopy, X-ray diffraction, and thermogravimetric analysis. By inserting a flexible spacer between the mesogenic core and the terminal menthyl groups, mesomorphism of $\mathbf{M_{LC}}$ was realized. $\mathbf{LCE_1}$–$\mathbf{LCE_4}$ with low content of crosslinking unit exhibited cholesteric phase because of the introduction of the nematic crosslinking unit. This indicates that low levels of chemical crosslinking do not significantly affect the phase behavior and mesomorphism of the elastomers, and reversible mesophase transitions can be observed. In addition, with increasing the content of crosslinking unit, the corresponding T_g decreased for $\mathbf{LCE_1}$–$\mathbf{LCE_4}$, whereas their T_i did not remarkable change. © 2012 Wiley Periodicals, Inc. J Appl Polym Sci 000: 000–000, 2012

Key words: phase behavior; crosslinking; liquid crystalline; elastomers; menthyl

INTRODUCTION

As a novel class of liquid crystalline (LC) materials, cholesteric elastomers have recently attracted theoretical and experimental interest because they give rise to new macroscopic features, which make them candidates for several applications, such as electro-optical switches, switchable color-tunable reflectors, full-color reflective displays, and artificial muscles.[1–6] From a scientific point of view, liquid crystalline elastomers (LCEs) are fascinating because they combine rubber elasticity and mechanical characteristics of lightly crosslinked polymer networks chains with the orientational order and variable optical birefringence of LC phases.[7–18] As a result, they show a complicated response to mechanical strain, because the conformational changes of polymer chains affect the LC order. They have complex mechanical behavior arising from the coupling of the orientational degrees of freedom of the mesogenic order and those of the rubber-elastic matrix and show remarkable elastic properties, because the polymer conformations are biased along LC director.

Similar to nematic and smectic elastomers, cholesteric elastomers not only hold the entropic elasticity but also show reversible LC phase transitions during heating and subsequent cooling. Besides conventional electro-optical and mechanical properties, cholesteric elastomers show piezoelectricity, tunable lasing, and photonics.[19–24] They have the potential to act as a device that transforms a mechanical signal into an electric signal when stress is applied parallel to the cholesteric helix, and they are considered as a candidate for the piezoelectric device.

Menthol derivatives have been used as a nonmesogenic chiral monomer for the synthesis of side chain chiral LC copolymers.[25–30] However, to the best of our knowledge, research on LC monomers, homopolymers and elastomers based on menthyl groups had not been reported. We found that LC phase of chiral compounds containing menthyl groups can be realized by inserting a flexible spacer between the mesogenic core and the bulky terminal menthyl fragments. In this study, the synthesis of new cholesteric monomer and elastomers containing menthyl groups is reported. Their phase behavior and mesomorphism were investigated with differential scanning calorimetry (DSC), polarizing optical microscopy (POM), thermogravimetric analysis (TGA), and X-ray diffraction (XRD). The selective reflection of light was studied with UV/visible/NIR. The effect of the content of the crosslinking units on

Correspondence to: J.-S. Hu (hujs@mail.neu.edu.cn).
Contract grant sponsor: Science and Technology Bureau of Shenyang.
Contract grant sponsor: Fundamental Research Funds for the Central Universities; contract grant numbers: N090505002, N090105001.

phase behavior and mesomorphism of the elastomers was investigated.

EXPERIMENTAL

Materials

L-Menthol was purchased from Shanghai Kabo Chemical (Shanghai, China). Chloroacetic acid was purchased from Tianjin Bodi Chemical (Tianjin, China). Hexamethylene chlorohydrin was purchased from Zhouping Mingxing Chemical Engineering (Zhouping, China). 4-Hydroxybenzoic acid was obtained from Shanghai Wulian Chemical Plant (Shanghai, China). Undec-10-enoic acid was purchased from Beijing Jinlong chemical Reagent (Beijing, China). 4,4′-Dihydroxybiphenyl (from Aldrich) was used as received. Polymethylhydrosiloxane (PMHS, DP = 6) was purchased from Jilin Chemical Industry (Jilin, China). All other solvents and reagents used were purified by standard methods.

Characterization

FTIR spectra were measured on a PerkinElmer spectrum One (B) spectrometer (PerkinElmer, Foster City, CA). ^{1}H-NMR spectra were obtained with a Bruker ARX400 spectrometer (Bruker, Swiss). The elemental analyses were carried out with an Elementar Vario EL III (Elementar, Hanau, Germany). The special optical rotations were obtained on a PerkinElmer 341 polarimeter. The phase behavior was determined with a Netzsch DSC 204 (Netzsch, Hanau, Germany) equipped with a cooling system. The heating and cooling rates were 10°C/min. The mesomorphism was observed with a Leica DMRX POM (Leica, Germany) equipped with a Linkam THMSE-600 (Linkam, UK) cool and hot stage. The thermal stability of the polymers and elastomers under nitrogen atmosphere was measured with a Netzsch TGA 209C thermogravimetric analyzer. The heating rates were 20°C/min. XRD measurements were performed with a nickel-filtered Cu-K_α (λ = 1.542 Å) radiation with a DMAX-3A Rigaku (Rigaku, Japan) powder diffractometer.

Synthesis of the intermediate compounds

The synthetic route of the intermediate compounds is outlined in Scheme 1. Menthyloxyacetic acid (**1**) and 4-(6-hydroxyhexyloxy)benzoic acid (**3**) were prepared according to the method reported by Hu et al.[31,32]

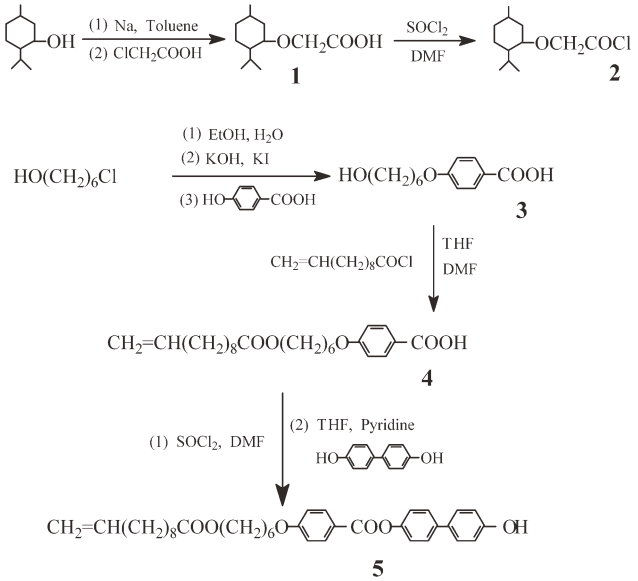

Scheme 1 Synthetic route of the intermediate compounds **1**–**5.**

4-(6-(Undec-10-enoyloxy)hexyloxy)benzoic acid (4)

Undecylenyl chloride (12.2 g, 55 mmol) was added dropwise to a solution of compound **3** (11.9 g, 50 mmol) in 150 mL of tetrahydrofuran (THF) and 5 mL of *N*,*N*-dimethylformamide (DMF). The mixture was reacted for 2 h at room temperature and 20 h at 60°C. After the reaction mixture was concentrated, and then the crude product was precipitated by adding water to the residue. The solid **4** was obtained by recrystallization from ethanol. Yield: 80%, mp: 89°C.

IR (KBr): 2928, 2853 (—CH_2—); 2673, 2563 (—COOH); 1728, 1688 (C=O); 1641 (C=C); 1607, 1514 (Ar-), 1255 cm^{-1} (C—O—C).

^{1}H-NMR ($CDCl_3$, TMS, δ, ppm): 1.35–1.82 [m, 20H, CH_2=CHC***H***$_2$(C***H***$_2$)$_6$C***H***$_2$— and —COOC***H***$_2$(C***H***$_2$)$_4$C***H***$_2$O—]; 2.10 [m, 2H, CH_2=CHC***H***$_2$(CH_2)$_7$—]; 2.65 [m, 2H, CH_2=CH(CH_2)$_7$C***H***$_2$—]; 4.05 [t, 2H, —COO(CH_2)$_5$C***H***$_2$O—]; 4.13 [t, 2H, —COOC***H***$_2$(CH_2)$_5$O—]; 4.95–5.03 (m, 2H, C***H***$_2$=CH—); 5.77–6.90 (m, 1H, CH_2=C***H***—); 6.97–8.03 (m, 4H, Ar-***H***); 10.9 (s, 1H, —COO***H***).

Elem. Anal. Calcd. for $C_{24}H_{36}O_5$: C, 71.26%; H, 8.97%. Found: C, 71.41%; H, 9.06%.

4-Hydroxybiphenyl-4′-(6-(undec-10-enoyloxy) hexyloxy)benzoate (5)

4-(2-Undec-10-enoyloxyhexyloxy)benzoyl chloride was prepared through the reaction of **4** with excess thionyl chloride. The acid chloride obtained (6.3 g, 15 mmol) was added dropwise to a solution of 4,4′-dihydroxybiphenyl (9.3 g, 50 mmol) in 100 mL of THF and 1 mL of pyridine. The mixture was reacted for 6 h at room temperature and for 8 h at 65°C. After the reaction mixture was concentrated, the crude product was precipitated by adding ice-water to the residue, and washed with 2% NaOH solution, then

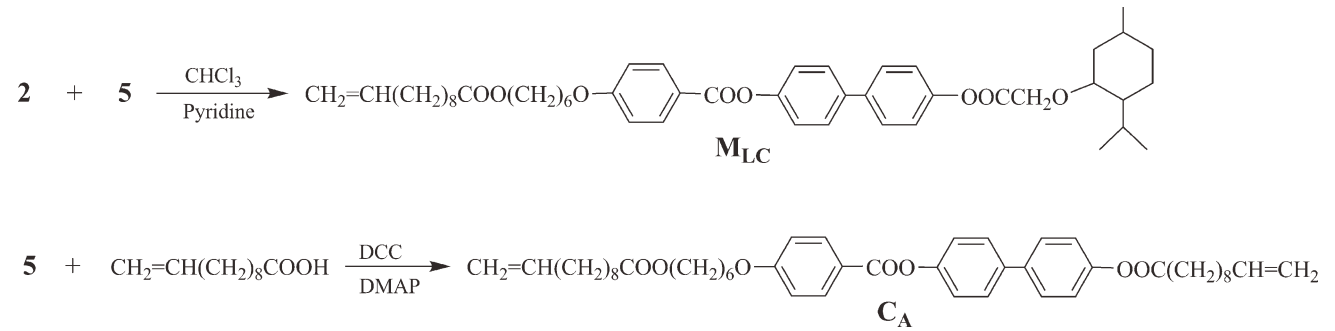

Scheme 2 Synthetic route of the chiral monomer $\mathbf{M_{LC}}$ and crosslinking agent $\mathbf{C_A}$.

neutralized with diluted HCl. The solid **5** was obtained by recrystallization from ethanol/acetone (3 : 2). Yield: 42%, mp: 136°C.

IR (KBr): 3461 (—OH); 2927, 2854 (—CH_2—); 1732 (C=O); 1641 (C=C); 1608, 1498 (Ar—), 1261cm^{-1} (C—O—C).

^{1}H-NMR ($CDCl_3$, TMS, δ, ppm): 1.36–1.83 [m, 20H, CH_2=CHC***H***$_2$($C\mathbf{H}_2$)$_6$$CH_2$— and —COOC$H_2$($C\mathbf{H}_2$)$_4$$CH_2$O—]; 2.09 [m, 2H, CH_2=CHC***H***$_2$$(CH_2)_7$—]; 2.64 [m, 2H, CH_2=CH$(CH_2)_7$C***H***$_2$—]; 4.06 [t, 2H, —COO$(CH_2)_5$C***H***$_2$O—]; 4.15 [t, 2H, —COOC***H***$_2$$(CH_2)_5$O—]; 4.97–5.04 (m, 2H, C***H***$_2$=CH—); 5.76–6.90 (m, 1H, CH_2=C***H***—); 6.96–8.01 (m, 12H, Ar-***H***); 5.3 (s, 1H, —O***H***).

Elem. Anal. Calcd. for $C_{36}H_{44}O_6$: C, 75.50%; H, 7.74%. Found: C, 75.62%; H, 7.81%.

Synthesis of the chiral monomer and crosslinking agent

The synthetic route for the chiral monomer $\mathbf{M_{LC}}$ and crosslinking agent $\mathbf{C_A}$ is outlined in Scheme 2.

4-(Menthyloxyacetoxy)biphenyl-4′-(6-(undec-10-enoyloxy)hexyloxy)benzoate (M_{LC})

The compound **2** (2.55g, 11 mmol), dissolved in 5 mL of chloroform, was added to stirred solution of the compound **5** (5.72 g, 10 mmol) in 30 mL of chloroform and 1 mL of pyridine. The mixture was refluxed for 24 h, cooled to room temperature, filtered, and then concentrated. The crude product was precipitated by adding methanol to the filtrate, purified by column chromatography (silica gel, dichloromenthane). Yield: 49%. mp: 63°C.

IR (KBr): 2929, 2869 (CH_3—, —CH_2—); 1776, 1728 (C=O); 1641 (C=C); 1604–1492 (Ar-); 1207cm^{-1} (C—O—C).

^{1}H-NMR ($CDCl_3$, TMS, δ): 0.79–2.65 [m, 42H, —($C\mathbf{H}_2$)$_8$—, —COOCH_2($C\mathbf{H}_2$)$_4$$CH_2$O— and in menthyl-***H***]; 3.27–3.36 (m, 1H, —C***H***< in menthyl); 4.06–4.14 [m, 4H, —COOC***H***$_2$$(CH_2)_4$C***H***$_2$O—]; 4.37–4.48 (m, 2H, —OOCC***H***$_2$O—); 4.93–5.04 (m, 2H, C***H***$_2$=); 5.76–5.90 (m, 1H, =C***H***—); 6.99–8.20 (m, 12H, Ar-***H***).

Elem. Anal. calcd for $C_{48}H_{64}O_8$: C, 74.97%; H, 8.39%. Found: C, 74.86%; H, 8.48%.

4-(Undec-10-enoyloxy)biphenyl-4′-(6-(undec-10-enoyloxy)hexyloxy)benzoate (C_A)

The compound **5** (5.72 g, 10 mmol), dissolved in 80 mL of dry dichloromethane, were added to 20 mL of dichloromethane solution containing undec-10-enoic acid (2.21 g, 12 mmol), *N*,*N*′-dicyclohexyl carbodiimide (DCC; 2.47 g, 12 mmol), and *N*, *N*′-dimethylaminopyridine (DMAP; 0.12 g, 1 mmol). The reaction mixture was stirred for 30 h at 30°C. The resulting solution was washed with 10 mL of water, stirred for 0.5 h, and filtered. After removing the water, the organic layer was dried with anhydrous magnesium sulfate and evaporated to dryness. The crude product was purified by column chromatography (silica gel, dichloromenthane). White solid was obtained. Yield: 81%. mp: 55°C.

IR (KBr): 2924, 2852 (—CH_2—); 1749, 1732 (C=O); 1641 (C=C); 1606–1494 (Ar-); 1270cm^{-1} (C—O—C).

^{1}H-NMR ($CDCl_3$, TMS, δ): 1.28–2.35 [m, 40H, —($C\mathbf{H}_2$)$_8$— and —COOCH_2($C\mathbf{H}_2$)$_4$$CH_2$O—]; 4.06–4.14 [m, 4H, —COOC***H***$_2$$(CH_2)_4$C***H***$_2$O—]; 4.94–5.06 (m, 4H, C***H***$_2$=); 5.76–5.91 (m, 2H, =C***H***—); 6.99–8.20 (m, 12H, Ar-***H***).

Elem. Anal. calcd for $C_{47}H_{62}O_7$: C, 76.39%; H, 8.46%. Found: C, 76.51%; H 8.59%.

Synthesis of the elastomers

The elastomers $\mathbf{LCE_1}$–$\mathbf{LCE_4}$ were synthesized through same method. The synthesis of $\mathbf{LCE_1}$ is described as follows. $\mathbf{M_{LC}}$ (1.06 g, 1.38 mmol), $\mathbf{C_A}$ (0.04 g, 0.06 mmol) and **PMHS** (0.17 g, 0.25 mmol) were dissolved in 30 mL of dry toluene. The reaction mixture was heated to 65–70°C under nitrogen and anhydrous conditions, and then 2 mL of THF solution with the H_2PtCl_6 catalyst (5 mg/mL) was injected into mixture with a syringe. The progress of the hydrosilylation reaction, monitored by the Si—H stretch intensity, went to completion, as indicated by IR. $\mathbf{LCE_1}$ was obtained by precipitation from toluene

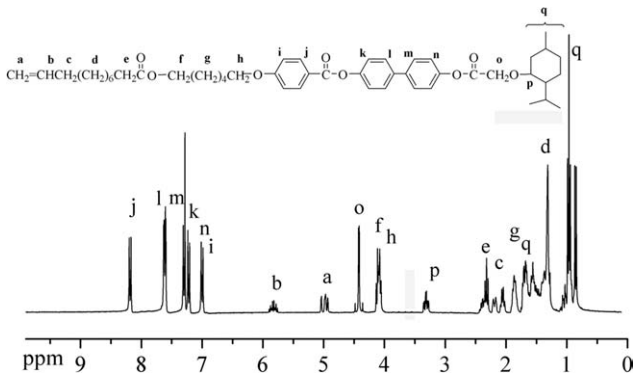

Figure 1 ^{1}H NMR spectrum of chiral monomer $\mathbf{M_{LC}}$.

solution into methanol, purified by several filtrations from hot ethanol, and then dried *in vacuo*.

IR (KBr, cm^{-1}): 2924, 2854 (—CH_3, —CH_2—); 1782, 1735 (C=O); 1606, 1494 (Ar-); 1270−1006 (Si—O—Si, C—Si and C—O—C).

RESULTS AND DISCUSSION

Synthesis

The structures of the target chiral monomer $\mathbf{M_{LC}}$ and crosslinking agent $\mathbf{C_A}$ were characterized by FTIR and ^{1}H-NMR. IR spectra of $\mathbf{M_{LC}}$ and $\mathbf{C_A}$ showed characteristic stretching bands at 1776 cm^{-1} attributed to ester C=O in menthyloxyacetate, 1749 and 1641cm^{-1} attributed to ester C=O, and double bond C=C in undec-10-enoyl and 1732−1728 cm^{-1} attributed to ester C=O in substituted benzoate. ^{1}H-NMR spectra of $\mathbf{M_{LC}}$ and $\mathbf{C_A}$ showed multiplet at 5.92−4.92 ppm corresponding to olefinic protons in undecenoyl. ^{1}H-NMR spectra of $\mathbf{M_{LC}}$ are shown in Figure 1. The spectra suggest that the chemical structures of $\mathbf{M_{LC}}$ and $\mathbf{C_A}$ are consistent with the designed and expected molecular structures.

The elastomers $\mathbf{LCE_1}$−$\mathbf{LCE_4}$ were prepared by a one-step hydrosilylation reaction using hexchloroplatinate hydrate as catalyst at 70°C. The polymerization feed and yields were shown in Table I. IR spectra of $\mathbf{LCE_1}$−$\mathbf{LCE_4}$ showed the complete disappearance of the Si—H stretching band at 2166 cm^{-1} and olefinic C=C stretching band at 1641 cm^{-1}. Characteristic Si—C bands appeared at about 1270 and 778 cm^{-1} and Si—O—Si bands appeared at about 1203, 1167, 1117, 1071, and 1006 cm^{-1}. In addition, the typical absorption bands of ester C=O and aromatic still existed.

Phase behavior and mesomorphism of monomer and crosslinking agent

The phase behavior and mesomorphism of $\mathbf{M_{LC}}$ and $\mathbf{C_A}$ were investigated with DSC and POM. Their phase transition temperatures are summarized in Table II. Typical DSC curves of $\mathbf{M_{LC}}$ are shown in Figure 2.

DSC curves of $\mathbf{M_{LC}}$ showed a melting transition at 63.0°C and a cholesteric to isotropic phase transition at 81.1°C on heating and an isotropic to cholesteric phase transition at 79.6°C and a crystallization transition at 5.1°C on cooling. POM result showed that $\mathbf{M_{LC}}$ exhibited enantiotropic oily streak texture and focal conic texture; moreover, the focal conic texture easily transformed to oily steak texture due to macroscopic orientation of the domains by shearing this mesophase, which is typical characteristic of cholesteric LC. The optical textures of $\mathbf{M_{LC}}$ are shown in Figure 3(a,b).

The unique optical properties of cholesteric LC are related to their helical supermolecular structure. The periodic helical structure selectively reflects visible light like an ordinary diffraction grating. The selective reflection of light for $\mathbf{M_{LC}}$ was observed and shifted to the short wavelength region (blue shift) with increasing temperature. In order to describe the relationships of the maximun selective reflection wavelength of light (λ_m) and temperature, λ_m of $\mathbf{M_{LC}}$ was measured by UV/vis/NIR spectra with hot stage. Figure 4 shows UV/vis spectra of $\mathbf{M_{LC}}$ with temperature. λ_m decreased from 545 nm at 65°C to 505 nm at 75°C at cholesteric phase.

DSC curves of $\mathbf{C_A}$ showed three endothermic peaks, which represent a melting transition, a smectic A (S_A) to nematic phase transition, and a nematic to isotropic phase transition, respectively. On cooling, two exothermic peaks occurred, which represent

TABLE I
Yield, Polymerization, and Solubility

	Feed (mmol)			C_A[a]	Yield	Solubility
Elastomer	PHMS	M_{LC}	C_A	(mol %)	(%)	Toluene
$\mathbf{LCP_0}$	0.50	3.00	0	0	89	+
$\mathbf{LCE_1}$	0.50	2.76	0.12	4	87	−
$\mathbf{LCE_2}$	0.50	2.52	0.24	8	88	−
$\mathbf{LCE_3}$	0.50	2.40	0.30	10	85	−
$\mathbf{LCE_4}$	0.50	2.28	0.36	12	85	−

[a] Molar fraction of $\mathbf{C_A}$ based on ($\mathbf{M_{LC}}$ + 2$\mathbf{C_A}$); + soluble; − insoluble or swelling.

TABLE II
The Phase Transition Temperatures of Monomer and Crosslinking Agent

Monomer	$[\alpha]_D^{25}$[a]	Mesophase, phase transition temperature (°C), and enthalpy changes (J g^{-1})	
		Heating cycle	Cooling cycle
$\mathbf{M_{LC}}$	−37.9	K63.0(38.8)Ch81.1(3.5)I	I79.6(3.5)Ch5.1(2.9)K
$\mathbf{C_A}$	–	K54.7(51.3)S_A96.2(6.6)N142.2(8.5)I	I140.7(8.4)N92.6(5.8)S_A−K

K = solid; Ch = cholesteric phase; S_A = smectic A phase; N = nematic; I = isotropic.
[a] Specific optical rotation, 0.21 g in 100 mL of $CHCl_3$.

an isotropic to nematic phase transition and a nematic to S_A phase transition; however, a crystallization transition peak was not seen because of supercooling phenomenon. POM results showed that $\mathbf{C_A}$ exhibited typical enantiotropic fan-shaped texture of a S_A phase and thread or schlieren texture of a nematic phase. The optical textures of $\mathbf{C_A}$ are shown in Figure 5(a,b).

In other words, all phase transitions for $\mathbf{M_{LC}}$ and $\mathbf{C_A}$ are reversible, and the transition temperatures noted with DSC are consistent with those observed by POM.

Phase behavior and mesomorphism of elastomers

The phase behavior, mesomorphism, and thermal stability of $\mathbf{LCE_1}$−$\mathbf{LCE_4}$ were investigated with DSC, POM, XRD, and TGA. The corresponding phase transition temperatures and thermal decomposition temperature are summarized in Table III. Typical DSC curves of $\mathbf{LCE_1}$−$\mathbf{LCE_4}$ are presented in Figure 6.

In general, the phase behavior and mesomorphism of side-chain LCEs mainly depend on the polymer backbone, copolymerization composition, and crosslinking density. For $\mathbf{LCE_1}$−$\mathbf{LCE_4}$, because of the same polysiloxanes backbone, the corresponding phase transition temperatures and mesomorphism mainly depend on the copolymerization composition and crosslinking density. If the copolymerization composition changed, the crosslinking density also changed, for example, when the content of crosslinking unit in elastomers increased, the corresponding crosslinking density also increased. Lightly crosslinked liquid crystalline polymers (LCPs) or LCEs with low crosslinking density may show the basic

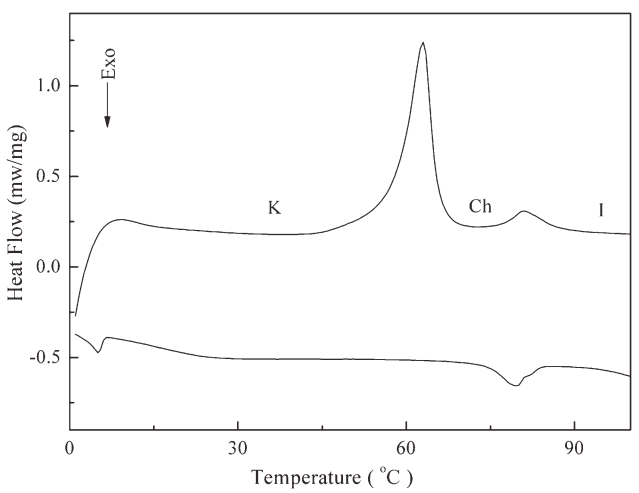

Figure 2 DSC curves of chiral monomer $\mathbf{M_{LC}}$.

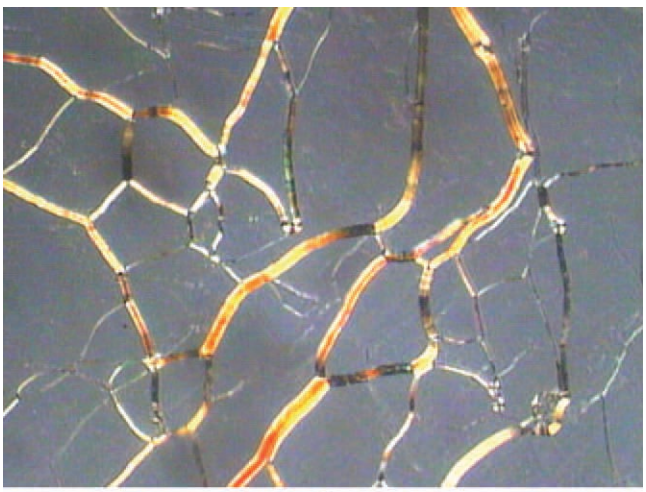

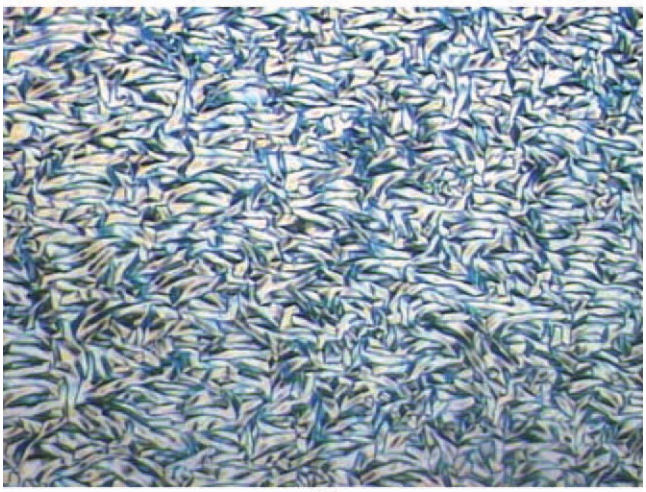

Figure 3 Optical textures of $\mathbf{M_{LC}}$ (200×). (a) Oily streak texture on heating to 80.5°C; (b) focal conic texture on cooling to 79.3°C. [Color figure can be viewed in the online issue, which is available at wileyonlinelibrary.com.]

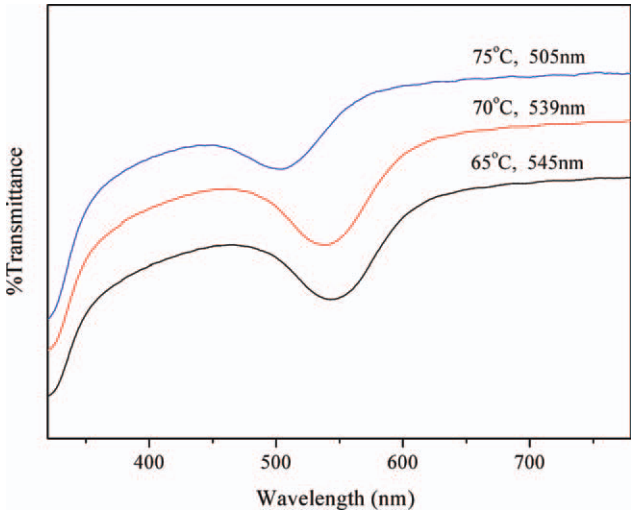

Figure 4 UV/Vis spectra of $\mathbf{M_{LC}}$ at mesophase. [Color figure can be viewed in the online issue, which is available at wileyonlinelibrary.com.]

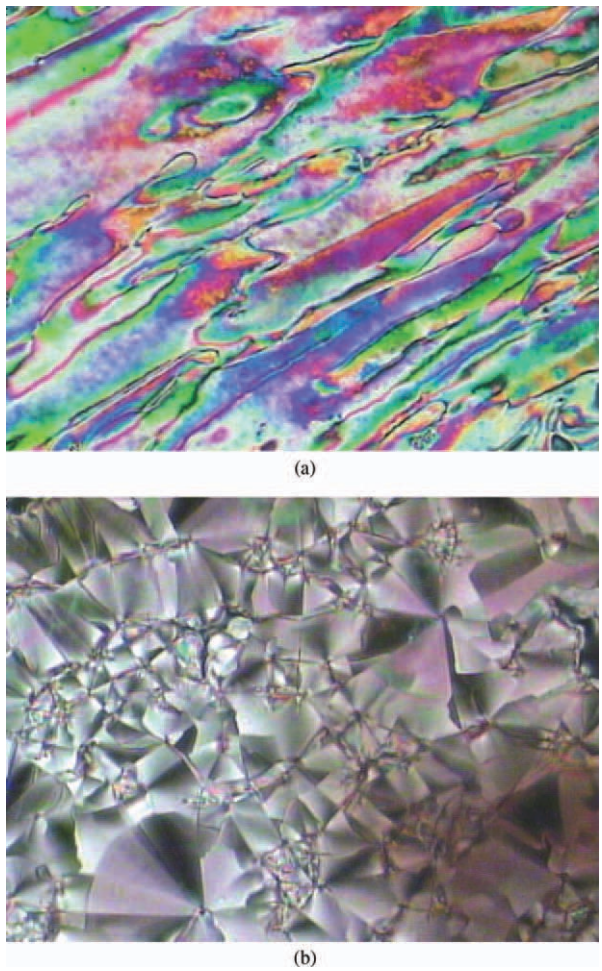

Figure 5 Optical textures of $\mathbf{C_A}$ (200×). (a) Thread texture of nematic phase on heating to 126.7°C; (b) fan-shaped texture of $\mathbf{S_A}$ phase on cooling to 86.9°C. [Color figure can be viewed in the online issue, which is available at wileyonlinelibrary.com.]

TABLE III
The Phase Transition Temperatures and Decomposition Temperatures of Elastomers

Elastomer	T_g (°C)	T_i (°C)	ΔH_i (J g^{-1})	ΔT[a]	T_d (°C)
LCP_0	16.5	124.1	3.0	107.6	339
LCE_1	5.5	121.5	3.7	116.0	329
LCE_2	1.6	119.2	2.6	117.6	325
LCE_3	1.7	123.4	2.4	121.7	330
LCE_4	0.5	122.3	2.8	121.8	332

[a] Mesophase temperature range (T_i–T_g).

features of polymeric networks with anisotropic physical properties coming from their LC phases with reversible phase transition during heating and cooling cycle. According to Figure 6, **LCE_1**–**LCE_4** all showed a glass transition and LC to isotropic phase transition. Moreover, POM showed that they exhibited the mesomorphism. This indicates that low levels of chemical crosslinking do not significantly affect their phase behavior, and reversible LC phase transitions can be observed because of enough mesogenic molecular motion.

It is known that chemical crosslinking imposes additional constraints on the motion of chain segments, makes free volume reduce, and causes an increase in the glass transition temperature (T_g). However, the effect may be small for lightly crosslinked polymers containing the flexible crosslinking unit with long spacer, and T_g is also affected by the flexible crosslinking chains similar to the plasticization effect. So, T_g of lightly crosslinked polymers may fall. According to Table III, T_g decreased from 16.5°C for uncrosslinked parent polymer **LCP_0** to 0.5°C for **LCE_4**.

POM results showed that **LCE_1**–**LCE_3** exhibited Grandjean texture of cholesteric phase because of the introduction of the nematic crosslinking unit.

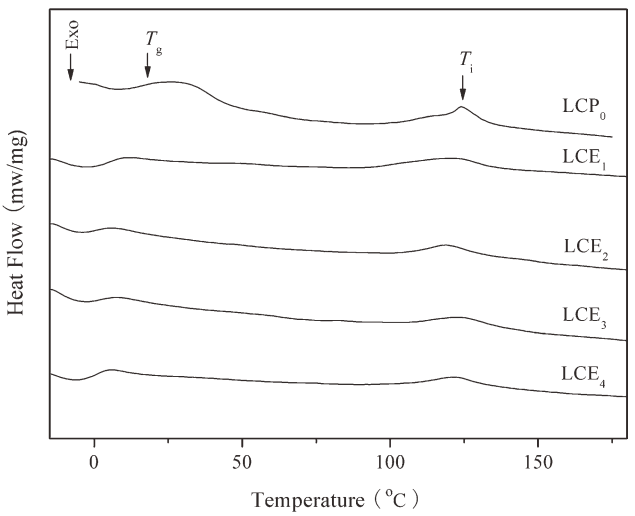

Figure 6 DSC curves of **LCP_0** and **LCE_1**–**LCE_4**.

LCE_4 exhibited stress-induced birefringence and good elasticity. For **LCE_1**−**LCE_4**, no sharp peak associated with the smectic layers appeared in small-angle X-ray scattering curves, however, a broad peak associated with the lateral packing occurred at $2\theta = 18–20^\circ$. Therefore, cholesteric structure of **LCE_1**−**LCE_4** was confirmed with POM and XRD.

TGA showed that the temperatures at which 5% weight loss occurred (T_d) were greater than 325°C, this indicates that **LCE_1**−**LCE_4** had a good thermal stability.

CONCLUSIONS

The synthesis and phase behavior of new cholesteric monomer and elastomers containing menthyl groups are reported. By inserting a flexible spacer between the mesogenic core and the bulky terminal menthyl fragments to reduce steric hindrance effect, the mesomorphism of the compound based on menthyl groups can be realized. The monomer **M_{LC}** showed cholesteric phase, and the crosslinking agent **C_A** showed S_A and nematic phases. The elastomers **LCE_1**−**LCE_4** exhibited cholesteric phase. When the content of crosslinking unit increased from 2 to 12 mol %, T_g decreased from 16.5°C for **LCP_0** to 0.5°C for **LCE_4**, whereas T_i did not remarkable change. In addition, **LCE_1**−**LCE_4** showed good thermal stability. Moreover, a flexible polysiloxane backbone, a rigid mesogenic core, a long spacer and low crosslinking density tended to exhibit a low glass transition temperature, wide mesophase temperature range, and high thermal stability.

References

1. Finkelmann, H.; Kim, S. T.; Munoz, A.; Palffy-Muhoray, P.; Taheri, B. Adv Mater 2001, 13, 1069.
2. Schmidtke, J.; Kniesel, S.; Finkelmann, H. Macromolecules 2005, 38, 1357.
3. Callan-Jones, A. C.; Pelcovits, R. A.; Meyer, R. B.; Bower, A. F. Phys Rev E 2007, 75, 011701.
4. Hirota1, Y.; Ji, Y.; Serra, F.; Tajbakhsh, A. R.; Terentjev1, E. M. Opt Exp 2008, 16, 5320.
5. Yang, H.; Buguin, A.; Taulemesse, J. M.; Kaneko, K.; Mery, S.; Bergeret, A.; Keller, P. J Am Chem Soc 2009, 131, 15000.
6. Ohm, C.; Brehmer, M.; Zentel, R. Adv Mater 2010, 22, 3366.
7. Jahromi, S.; Lub, J.; Mol, G. N. Polymer 1994, 35, 622.
8. Ortiz, C.; Ober, C. K.; Kramer, E. J. Polymer 1998, 39, 3713.
9. Hsu, C. S.; Chen, H. L. J Polym Sci Part A: Polym Chem 1999, 37, 3929.
10. Li, M.; Hu, Z. J.; Chen, G.; Chen, X. F. J Appl Polym Sci 2003, 88, 2275.
11. Arai, Y. O.; Urayama, K.; Kohjiya, S. Polymer 2004, 45, 5127.
12. Saikrasun, S.; Bualek-Limcharoen, S.; Kohjiya, S.; Urayama, K. J Polym Sci Part B: Polym Phys 2005, 43, 135.
13. Hu, J, S.; Zhang, B. Y.; Zhou, A. J.; Yang, L. Q.; Wang, B. Euro Polym J 2006, 42, 2849.
14. Beyer, P.; Terentjev, E. M.; Zentel, R. Macromol Rapid Commun 2007, 28, 1485.
15. Ren, W.; Mcmullan, P. J.; Griffin, A. C. Macromol Chem Phys 2008, 209, 1896.
16. Tashiro, T.; Kondo, Y.; Hiraoka, K. Macromol Rapid Commun 2010, 31, 1948.
17. Ohm, C.; Haberkorn, N.; Theato, P.; Zentel, R. Small 2011, 7, 194.
18. Sanchez-Ferrer, A.; Finkelmann, H. Macromol Rapid Commun 2011, 32, 309.
19. Bunning, T. J.; Kreuzer, F. H. Trends Polym Sci 1995, 3, 318.
20. Palffy-Muhoray, P. Nature 1998, 391, 745.
21. Bermel, P. A.; Warner, M. Phys Rev E 2002, 65, 056614.
22. Castro-Garay, P.; Reyes, J. A.; Corella-Madueno, A. Appl Phys Lett 2009, 94, 163504.
23. Serra, F.; Matranga, M. A.; Ji, Y.; Terentjev, E. M. Opt Exp 2010, 18, 575.
24. Mota, A. E.; Palomares, L. O.; Reyes, J. A. Appl Phys Lett 2010, 96, 081906.
25. Mihara, T.; Nomura, K.; Funaki, K. Polym J 1997, 29, 309.
26. Altomare, A.; Andruzzi, L.; Ciardelli, F.; Gallot, B.; Solaro1, R. Polym Int 1998, 47, 419.
27. Bobrovsky, A. Y.; Shibaev, V. P. Adv Funct Mater 2002, 12, 367.
28. Hu, J. S.; Zhang, B. Y.; Pan, W.; Zhou, A. J. Liq Cryst 2005, 32, 441.
29. Liu, J. H.; Yang, P. C. Polymer 2006, 47, 4925.
30. Liu, J. H.; Hung, H. J.; Yang, P. C.; Tien, K. H. J Polym Sci Part A: Polym Chem 2008, 46, 6214.
31. Hu, J. S; Wei, K. Q.; Zhang, B. Y.; Yang, L. Q. Liq Cryst 2008, 35, 925.
32. Hu, J. S.; Zhang, B. Y.; Jia, Y. G.; Wang, Y. Polym J 2003, 35, 160.